Available online at www.sciencedirect.com
SCIENCE DIRECT®
PERGAMON
Applied Radiation and Isotopes 59 (2003) 263–266
Applied Radiation and Isotopes
www.elsevier.com/locate/apradiso

Determination of neutron flux distribution in an Am–Be irradiator using the MCNP

K. Shtejer-Diaz[a,b], C.B. Zamboni[b], G.S. Zahn[b,*], J.Y. Zevallos-Chávez[c]

[a] Center of Applied Studies for Nuclear Development, CEADEN, Calle 30, 502, Havana 6122, Cuba
[b] Instituto de Pesquisas Energéticas e Nucleares, IPEN/CNEN-SP, Rua do Matão, Travessa R, 400, 05508-900 São Paulo, Brazil
[c] Instituto de Física da Universidade de São Paulo—IFUSP, Rua do Matão, Travessa R, 187, 05508-900 São Paulo, Brazil

Received 11 February 2003; received in revised form 5 June 2003; accepted 24 June 2003

Abstract

A neutron irradiator has been assembled at IPEN facilities to perform qualitative–quantitative analysis of many materials using thermal and fast neutrons outside the nuclear reactor premises. To establish the prototype specifications, the neutron flux distribution and the absorbed dose rates were calculated using the MCNP computer code. These theoretical predictions then allow one to discuss the optimum irradiator design and its performance.

Keywords: MCNP; Neutron flux; Neutron dose

1. Introduction

The development of appropriate nuclear instrumentation to perform neutron activation analysis (NAA) using thermal as well as fast neutrons can be useful to investigate elements in a variety of sample matrices outside the reactor premises. Considering this fact, a small-sized neutron irradiator prototype is under construction at the IPEN facilities, in São Paulo.

The NAA can be divided into steps: first, the material to be analyzed (sample) and a standard are exposed to the thermal neutron flux of a nuclear reactor; afterwards, the induced activity in the sample is measured by the comparative method. The use of the neutron irradiator presents the advantage of supplying a stable neutron flux for a long period, thus eliminating the need for using standard material. This way the analyzing process became agile, practical and economic.

In this work the description of the neutron irradiator is presented and, according to those specifications, the neutron flux and absorbed dose rate distribution are calculated using the MCNP code (Briesmeister, 2000).

2. Neutron irradiator design

This prototype consists of an Aluminum cylinder of 5 mm thickness with 1200 mm length and 985 mm diameter, filled with paraffin, and two perpendicular cylindrical cavities (B and C) which cross at the prototype's geometric center. In the metallic cavity B (also of 5-mm-thick Aluminum, with an inner diameter of 80 mm) a ruler passes through the longitudinal direction, where the material to be irradiated can be put in different positions. In the cavity C (128 mm diameter, without Aluminum), the two neutron sources are positioned symmetrically, at the same distance from the geometric center, face to face.

The Americium–Beryllium (Am–Be) sources were commercially obtained and both have the following specifications: 600 GBq $^{241}Am^{9}Be$ (α, n) neutron source, with cylindrical design (40 mm diameter by 70 mm long) made of corrosion-resistant alloy. Taking into account that the specific source strength for $^{241}Am^{9}Be$ is

*Corresponding author. Tel.: +55-11-38169181; fax: +55-11-38169188.
E-mail address: gzahn@curiango.ipen.br (G.S. Zahn).

0969-8043/$ - see front matter
doi:10.1016/S0969-8043(03)00167-2

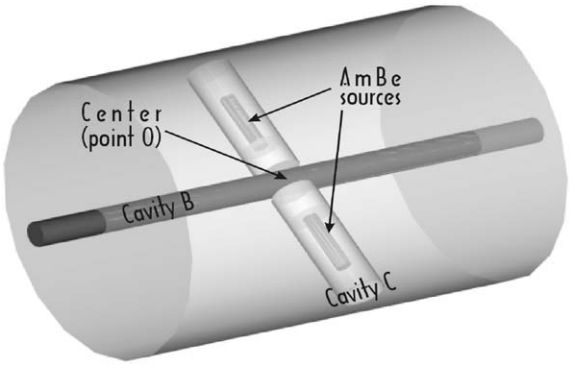

Fig. 1. Perspective view of the irradiator. Thermal neutrons are predominant configuration.

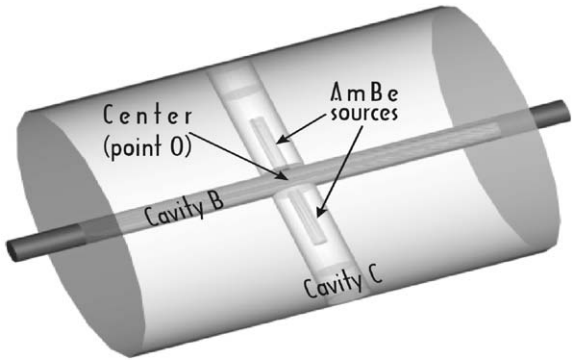

Fig. 2. Perspective view of the irradiator. Fast neutrons are predominant configuration.

6.6×10^{-5} n Bq^{-1} (International Organization for Standardization, 1989), each source has a neutron emission rate of 3.9×10^{7} n/s. Two different configurations, related to the neutron sources arrangements, can be explored:

(a) *Thermal neutrons prevalence*. In this situation, a 100 mm-long polyethylene cylinder is placed between each neutron source and the outer wall of cavity B in order to thermalize the emitted neutrons (Fig. 1);
(b) *Fast neutrons prevalence*. In this situation, the polyethylene cylinders are removed and the neutron sources are positioned 45 mm away from the prototype's geometrical center (Fig. 2).

3. Monte Carlo calculations

The MCNP code developed in Los Alamos (Briesmeister, 2000) carries out the radiation transport, relating to neutrons, photons and electrons with energetic and temporal dependence in a three-dimensional geometry by using the Monte Carlo method. This method is based in the probability distribution function for developing the random sampling of each event and performing the evolution of the particular phenomena being studied by means of convenient statistical techniques. The capabilities of this code involve the correct simulation of the physical problem and the geometrical configuration.

In this work, the MCNP-4C code was used to estimate the spatial distributions of flux that arise from the two different source configurations outlined earlier. The energy ranges considered were thermal below the cadmium cutoff energy (0.5 eV), epithermal (between 0.5 eV and 0.5 MeV) and fast neutrons (above 0.5 MeV).

For the neutron flux calculations, the tally F4:N was used. This tally allows the calculation of the flux average over a cell (particles/cm^2). In this Monte Carlo simulation, 5×10^6 histories were run, thus providing an estimated relative error less than 10%, producing reliable confidence intervals. Furthermore, other statistical parameters like figure of merit (FOM) were examined through fluctuation charts for each tally, to be sure that the tallies appeared statistically well-behaved. Small spherical scoring regions were created along the central axis of the cavity B, and were used for tallying purpose by using the tally segment card (FS). With this card there is no need for specifying the problem geometry with extra cells just for tallying.

The biased discrete energy distribution of the Am–Be sources is a probability density experimentally measured (Angioletto, 2000). In this measurement, the fast energy spectrum for energies starting from 1 up to 12 MeV coincides very well with other reported spectrum (Thonsom, 1965), but it also has a good description for neutron energies below 1 MeV, as a result of a combination of spectrometric measurements for fast and thermal neutron flux coming from the source, as well as MCNP calculations, in an experimental arrangement specifically designed for this purpose; the resultant spectrum goes from 0.025 eV to 12 MeV.

In our problem two isotropic Am–Be sources with the same cylindrical volume distribution were simulated. The uniform particle position sampling, which is given by EXT variable and a power law built-in function, $p(x) = c/x/a$ for the source radius values (RAD) with $a = 1$, are the provided defaults. This guarantees a uniform sampling in the source volume.

It is a neutron-only problem (MODE N) with a neutron lower energy at the MCNP default energy cutoff value (10^{-11} MeV). The flux and dose rates were calculated for energies ranging from the cutoff value up to 12 MeV.

No variance-reduction techniques were used, only conservative methods like a standard track length tally selection for cell flux estimate. This tally (F4) was

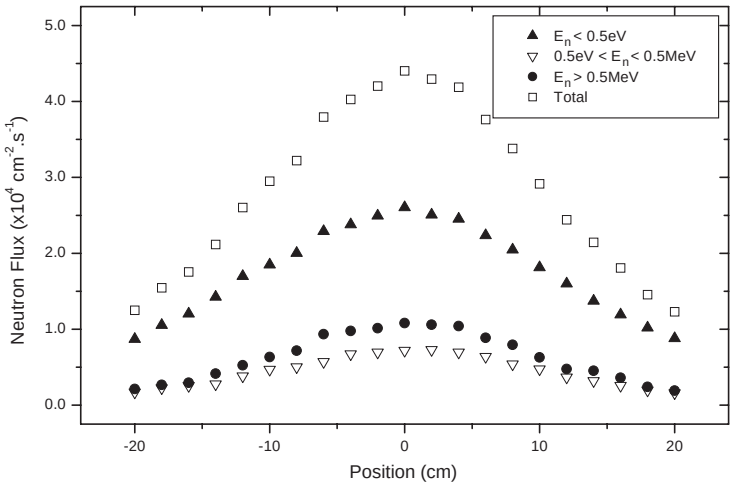

Fig. 3. Neutron flux distribution in the thermal configuration.

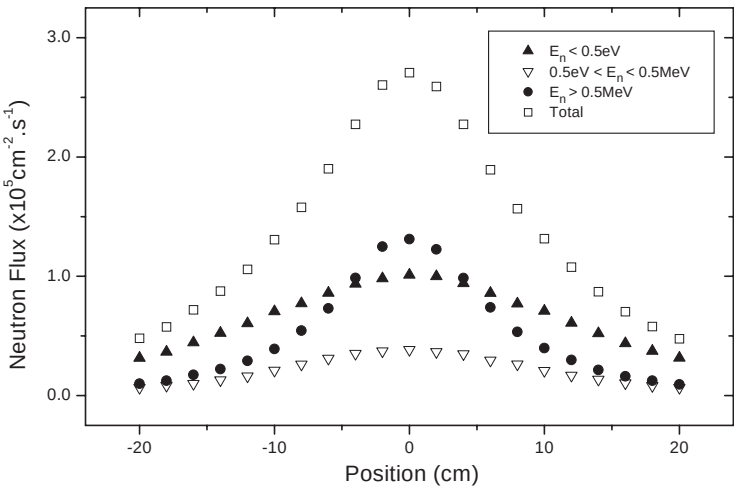

Fig. 4. Neutron flux distribution in the fast configuration.

carefully selected for avoiding high variance situations if one compares with tally F2 that gives a collision estimate of flux. In this work, all regions of the geometry were declared equally important regarding to particle transport. Only the outside space of the geometry has neutron importance equal to zero.

The results for the thermal-prevalence configuration are shown in Fig. 3 and the ones for the fast-prevalence one are in Fig. 4.

Particularly, for biological samples the knowledge of neutron dose rate is essential and this estimation can also be done using this code. The neutron absorbed dose rates for both configurations were calculated using the MCNP-4C code, and the results are shown in Figs. 5 and 6. In this work, the physical absorbed dose was estimated by calculating the neutron energy deposition average over the cell with tally F6:N. This is a track length estimate making possible the evaluation of the energy deposited per unit mass in any kind of material. Another work aimed to calculate the biological equivalent dose rates is under way. In this case flux-to-dose conversion factors will be estimated from TLD measurements and MCNP spectra simulations in each point of interest in our experimental arrangement because the reported sets of conversion factors from NCRP-38 (National Council on Radiation Protection and Measurements, 1971) and ICRP-21 (International Commission on Radiological Protection, 1971) in the MCNP code differ in some region of energies.

4. Discussion

The results presented in this work are important for a better knowledge of neutron flux distribution in the prototype. According to theoretical simulations, the

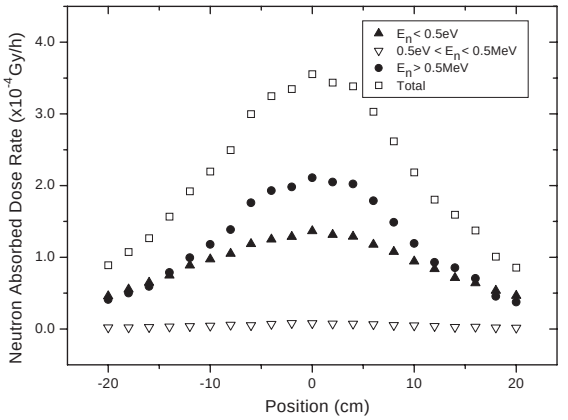

Fig. 5. Neutron absorbed dose rate, in thermal prevalence configuration, in different positions along the radial direction.

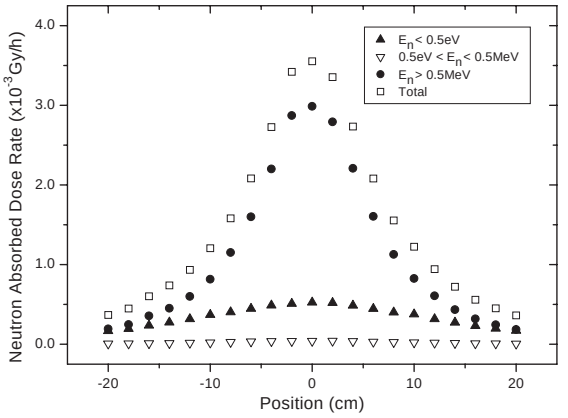

Fig. 6. Neutron absorbed dose rate, in fast prevalence configuration, in different positions along the radial direction.

prototype can be useful to investigate several biological, geological, metallic and ceramic samples. For biological samples, the prototype may be used to study stochastic effects of low neutron doses. It can also be used to test detectors, calibrate neutron dosimeters, and to do quality control check using NAA.

As an example of the possible uses for the prototype, Fig. 7 shows a plot of the estimated minimum mass detectable for some interest materials; for this estimate we assumed a maximum irradiation time of 7 days and the gamma-counting efficiency of a 70 cm^3 HPGe detector.

The main advantage of this irradiator is its very stable neutron flux that can be used to measure the induced activity in the specified material in an agile and economic way. Nevertheless, two points must be considered when analyzing this technique: the requirement of experienced radiological protection personnel to

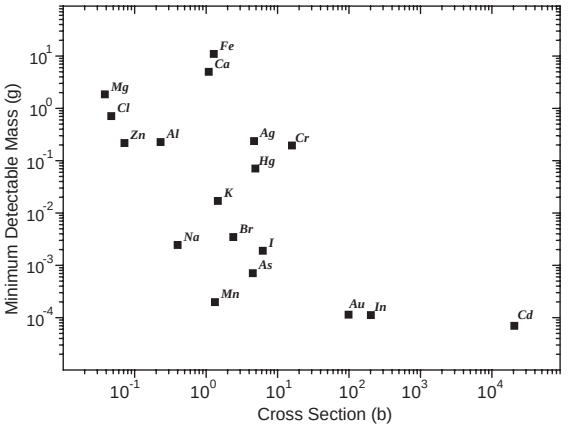

Fig. 7. Estimation of the minimum detectable mass for some material of interest.

perform the analysis outside the reactor premises; and the low neutron flux, when compared to a nuclear reactor, which will require large amounts of material when investigating a sample with low microscopic neutron cross section. This issue, however, may be addressed if there is enough sample material available, as the prototype can be used to irradiate up to several hundred grams of material—though this will require additional calculations, due to geometrical and self-absorption corrections.

Acknowledgements

The authors would like to thank the financial support from FAPESP, CNPq and CAPES.

References

Angioletto, E., 2000. Medidas e Cálculos de Espectro de Nêutrons Emergentes de Dutos em Blindagens. M.Sc. Thesis, IPEN, São Paulo, Brazil.

Briesmeister, J.F. (Ed.), 2000. MCNP—a general Monte Carlo N-particle transport Code. Version 4C, LA-13709 M.

International Commission on Radiological Protection, 1971. Data for protection against ionizing radiation from external sources: supplement to ICRP publication 15. ICRP-21.

International Organization for Standardization, 1989. Neutron reference radiations for calibrating neutron-measuring devices used for radiation protection purposes and for determining their response as a function of neutron energy. ISO 8259.

National Council on Radiation Protection and Measurements, 1971. Protection against neutron radiation. NCRP-38.

Thonsom, M.N., 1965. Neutron spectra from Am-α-Be and Ra-α-Be sources. Nucl. Instrum. Meas. 37, 305–308.